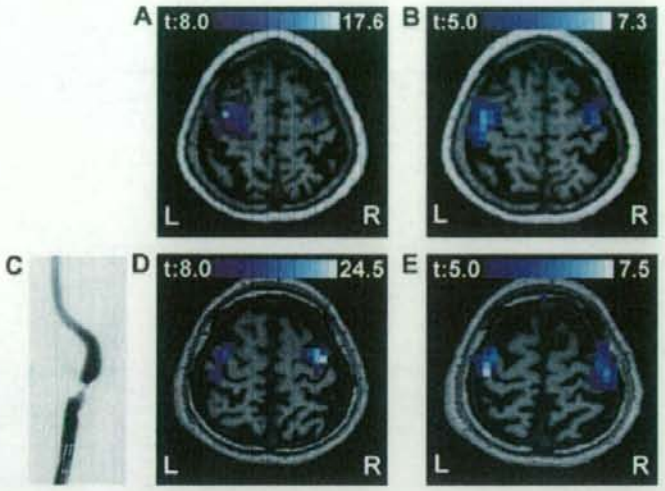

Figure 2. Voxels exhibiting statistically significant decrease in the power of β band (*t* value) are displayed in a blue scale. The images from a control subject (66-year-old woman) are shown as (A) (right hand grasping; Tc, 17.6; Ti, 11.3; LI, 0.22) and (B) (right finger-tapping; Tc, 7.3; Ti, 6.3; LI, 0.07). Both are classified as contralateral dominant pattern. C, The angiogram showing left carotid artery stenosis (80%) in patient 2 (65-year-old man). D, During right hand grasping in the same patient, the distribution pattern was classified as "ipsilateral-dominant" (Tc, 16.8; Ti, 24.8; LI, −0.18). E, In the same patient, a contralateral-dominant pattern (Tc, 7.5; Ti, 7.1; LI, 0.04) was seen during a right self-paced finger-tapping task.

power that indicates ERD was displayed in blue, whereas the power increase that indicates event-related synchronization (ERS) was shown in red. SAM statistical images were created for grasping and tapping tests with each hand giving 4 (2 for each task) images for each patient. Before SAM analysis, all trials were inspected visually. Data with sensors located in the most anterior or lower part of the helmet were excluded from analysis if they were accompanied by large artifacts caused by the presence of metal in the oral cavity (dental problems) or movements of eyeballs.

Patterns of Distribution of Beta Band Desynchronization

The laterality index (LI) was calculated using the peak *t* values around the sensorimotor area on contralateral and ipsilateral hemispheres with respect to the examined hand as follows: LI=(Tc−Ti)/(Tc+Ti),[13] where Tc is the highest peak *t* value on the contralateral hemisphere and Ti is that on the ipsilateral hemisphere. Based on the behavior of LI, we classified the spatial distribution of βERD into 3 types: contralateral-dominant (LI>0), bilaterally spread (−0.1≤LI≤0), and ipsilateral-dominant (LI<−0.1).

Evaluation of Sulcal Atrophy, Ventricular Size, and Periventricular White Matter Hyperintensity

The morphological changes in MR images of sulcal atrophy, ventricular size, and periventricular hyperintensity (PVH) of the hemisphere with the vascular lesion were assessed using a semiquantitative 10-point visual scale introduced by Manolio et al.[15] Three scorers, without any clinical information for patients, evaluated these 3 parameters. Sulcal atrophy and ventricular size were scored on T1-weighted images, and PVH was evaluated on FLAIR images (and not the proton images as in the original method of Manolio et al). Before analyzing the actual results, the 3 scorers performed a trial rating using MR images from a nonstudy patient and unified the scoring procedure. The variance in the visual scales among the 3 scorers was within 1 point for all parameters; hence, median values were calculated.

CBF Study With SPECT

Depending on their clinical conditions, the patients underwent [^{123}I] N-isopropyl-p-iodoamphetamine single-photon emission computed tomography (^{123}I-IMP SPECT) with or without an acetazolamide challenge test.[16] The details of SPECT procedure were reported previously.[16] Based on the neuroradiological reports, the degree of CBF impairment in the affected ICA or MCA region was categorized into 3 classes: no significant CBF reduction at rest (class A), CBF reduction at rest but with preserved vasoreactivity to acetazolamide (class B), and reduction at rest with impaired vasoreactivity (<23% increase) to acetazolamide as determined by a split-dose method (class C).[16]

Statistical Analysis

The results for age, Tc, Ti, and LI were analyzed with nonparametric Mann-Whitney *U* test. To compare the 2 groups of patients with respect to the presence or absence of ipsilateral dominant pattern, we used χ^2 with Fisher exact probability test. $P<0.05$ was considered as significant.

Results

Motor-Related Magnetic Fields in Control Subjects

In all control subjects, statistically determined regions of βERD with the highest *t* value were detected either on contralateral or ipsilateral sensorimotor, or premotor, cortex with respect to the examined hand (Figure 2A, B). The distribution patterns of βERD, peak *t* values (Tc and Ti), and LI during the 2 tasks are presented in Table 1. There was no evidence for the ipsilateral dominant distribution pattern of βERD, with the definition of LI <−0.1, in any individual in either of the tasks. Comparing the 2 tasks, the LI in hand grasping was larger than that in self-paced tapping, with an almost significant difference ($P=0.07$, Mann-Whitney *U* test). With respect to the side (right or left) of the examined hand, there were no significant differences in Ti, Tc, and LI

Table 1. Motor Magnetic Field Properties and βERD Distribution Patterns in Control Subjects

	Hand Grasping	Finger Tapping
Median Tc, range	13.6, 6.8–24.9	9.2, 6.0–14.2
Median Ti, range	7.5, 3.8–14.7	7.3, 3.2–11.0
Median LI, range	0.22,* −0.05–0.50	0.06, −0.05–0.38
Contralateral-dominant	15	14
Bilaterally spread	1	2
Ipsilateral-dominant	0	0

*$P=0.07$ with Mann-Whitney *U* test.
Results of 16 examinations (2×number of patients) are presented.

Table 2. Distribution Patterns of βERD in Patients With Vascular Occlusive Disease

Distribution Patterns	Hand Grasping	Finger Tapping
Median Tc, range	14.3, 2.8–32.3	7.6, 2.7–14.6
Median Ti , range	12.4, 5.2–25.3	6.3, 3.2–13.5
Median LI, range	0.10, −0.57–0.65	0.07, −0.19–0.37
Contralateral-dominant	53	49
Bilaterally spread	3	13
Ipsilateral-dominant	20	5

Median values (ranges) of Tc, Ti, LI, and the numbers in each distribution patterns are shown for 76 hand-grasping and 67 finger-tapping examinations.

in either tasks, although there was a slight tendency ($P=0.11$, Mann–Whitney U test) for the higher median Ti during left hand-grasping (9.7; range 6.7 to 14.3) as compared to right hand-grasping (7.4; range, 3.8 to 11.3).

Motor-Related Magnetic Fields in Patients With Occlusive Vascular Disease

In the group with atherosclerotic lesions (AS group), there were 21 men and 7 women, with an overall median age of 69 (range, 55 to 78) years; in that with nonatherosclerotic lesions (NAS group), median age was 48.5 (range, 21 to 73) and there were 4 men and 6 women. The age of the AS group was significantly higher than that of NAS ($P<0.05$, Mann-Whitney U test). According to the criteria for an "occlusive disease," 9 patients in the AS group and 4 (all with moyamoya disease) in the NAS group had bilateral lesions. The symptomatic side and, if asymptomatic, the side of the more severe stenosis or CBF reduction are listed as "the site" in supplemental Table I (available online at http://stroke.ahajournals.org). The location of a previous infarction and the presenting ischemic symptom are also given in the same Table.

All 76 hand-grasping examinations in 38 patients (ie, 1 per hand) were performed successfully. In finger-tapping, trials that contained occasional large noise or inadequate signals (eg, double taps in a trial) were eliminated. The number of excluded trials was ≈5%, with a maximum of 8 eliminated tapping trials in a single patient. However, 9 examinations of finger tapping were not available because of unforeseen problems with the measuring device in 2, injury of the relevant finger in 1, and inadequate performance attributable to sleepiness, or too-fast pacing in 6 (supplemental Table II) attributable to an unavailable cause. Therefore, 67 tapping and 76 hand-grasping examinations were analyzed.

As in control subjects, regions with the highest t values were detected around the contralateral or ipsilateral sensorimotor, or premotor, cortex (Figure 2D, E). The distribution pattern of βERD and values of Ti, Tc, and LI for 38 patients are shown in Table 2. It can be seen that 20 of 76 examinations during hand grasping and 5 of 67 examinations during tapping exhibited an ipsilateral-dominant βERD pattern. Results from either tasks were then analyzed separately for each hand (supplemental Table II). In 38 grasping examinations with the contralesional hand (or the more severe side for bilateral lesions), an ipsilateral-dominant pattern was observed in 16 of 28 examinations in the AS group, and in 1 of 10 in the NAS group. In grasping with the "other" hand, 25 of 38 examinations were in patients who showed no detectable lesions on the contralateral side, whereas the remaining 13 were with the contralesional hand in patients with bilateral lesions. In this latter set, the ipsilateral pattern was seen in 3 examinations, all of which were in the AS group. Summing up these results, during grasping task, the ipsilateral-dominant βERD pattern was seen in 20 examinations, 19 of which were in patients from the AS group and 1 was in a patient from the NAS group.

Table 3. Incidence of Ipsilateral-Dominant Pattern in Patients With Vascular Disease

	Ipsilateral-Dominant Pattern			
	Hand Grasping		Finger Tapping	
Condition	Present	Absent	Present	Absent
Contralesional hand	19†	32	3	42
Other side hand	1	24	2	20
AS group	19*	37	5	44
NAS group	1	19	0	18

*$P<0.05$ with χ^2 test with Yate correction.

†$P<0.01$ with χ^2 test with Yate correction.

AS group includes patients with atherosclerotic occlusive vascular lesion (n=28); NAS group, patients with nonatherosclerotic occlusive vascular lesion (n=10).

Values represent numbers of examinations. Nine of AS group and 4 of NAS had bilateral lesions, hence the number of examinations with contralesional hand in hand-grasping was 51 (38+13).

In the tapping task, the ipsilateral dominant βERD pattern was observed only in 5 examinations; all were from patients of the AS group (3 were with the "contralesional" and 2 were with the "other" hand).

Table 3 recalculates the results described by taking into consideration the fact that only 25 of 38 patients had no detectable lesion on the side contralateral to the "other" hand, whereas 13 had bilateral lesions. This increased the number of "contralesional hands" to 51. The new calculation shows that in the case of grasping, 19 of 51 examinations with the "contralesional" hand (18 in the AS group and 1 in the NAS group) showed the ipsilateral dominant βERD pattern, whereas the figure was only 1 (a patient in the AS group) of 25 for the other hand. When calculated for each group of patients, 19 of 56 examinations in the AS group (18 with the contralesional and 1 with the "other" hand) and 1 (with the contralesional hand) of 20 examinations in the NAS group exhibited this same pattern. In relation to the self-paced tapping task, the occurrence of an ipsilateral-dominant βERD pattern bore no significant relation to either the hand (contralesional or other) or etiology (AS or NAS group). A representative case that exhibited an ipsilateral-dominant pattern in hand-grasping but not in tapping with contralesional hand is shown (Figure 2).

Factors Related to an Ipsilateral-Dominant βERD Pattern in the Grasping Task With the Hand Contralateral to the Atherosclerotic Occlusive Vascular Lesions

Because the ipsilateral-dominant βERD pattern was observed significantly more frequently in grasping with the contrale-

Table 4. Relationship Between Clinical Factors and the Ipsilateral-Dominant Pattern in 37 Grasping Examinations With the Hand Contralateral to the Site of the Atherosclerotic Occlusive Vascular Lesions

	Ipsilateral-Dominant Pattern in Contralesional Hand Grasping		
Factor	Present	Absent	Significance
Age	70.5 (60–74)	60.5 (55–78)	$P<0.05$*
Tc	13.8 (5.2–25.9)	14.3 (7.0–25.1)	NS
Ti	23.7 (10.4–32.3)	9.9 (3.3–22.6)	$P<0.001$*
Score of sulcal atrophy	4 (2–7)	3 (2–6)	NS
Score of ventricular size	4 (1–7)	3 (1–6)	$P<0.05$*
Score of PVH	5.5 (2–7)	4 (1–7)	$P<0.01$*
Class C in CBF study (+/−)	7/11	6/9	NS
Ischemic event (+/−)	7/11	7/12	NS
Previous infarction (+/−)	3/15	4/15	NS
Side of the hand (left/right)	7/11	7/12	NS
Vascular lesion (MCA/ICA)	7/11	1/18	$P<0.05$†

*With Mann-Whitney U test.

†With χ^2 test with Fisher exact probability method.

Number for age was 16 in "present" and 12 in "absent" (28 patients in total). In all other comparisons number was 18 for the former and 19 for the latter, giving a total of 37 examinations. Relevant median values (ranges) are presented: Ti and Tc and peak t values on the ipsilateral and contralateral hemisphere, respectively.

sional hand in the AS group, we investigated the effect of several other "factors" on the frequency of this pattern (Table 4) in this same group. In 28 patients, 9 had bilateral lesions, resulting in 37 examinations of contralesional hand-grasping: 18 of these showed the ipsilateral βERD pattern, whereas 19 did not. Statistical analysis shows that the ipsilateral-dominant βERD pattern was seen more often in older patients and was accompanied by a higher Ti, but without a significantly different Tc. Scores for PVH and ventricular size on the side of the vascular lesion had higher values in cases that exhibited the dominant ipsilateral pattern. No significant relation was detected with respect to the incidence of "class C in CBF study," "history of ischemic event," "previous infarction" on the side of the vascular lesion, and the use of "left (nondominant) hand." However, "MCA lesion" as compared with "ICA lesion" showed a significant correlation with the appearance of the ipsilateral-dominant βERD pattern. Individual data of morphological changes in MR images, CBF state, and other "factors" on the vascular lesion side can be found in supplemental Table I.

Discussion

A significant asymmetry in motor-related cortical activity was detected with MEG during grasping with the hand contralateral to the side of an atherosclerotic occlusive vascular disease. The ipsilateral-dominant distribution of βERD was present significantly more frequently in older patients and in those with more severe morphological changes. We feel that this phenomenon, which occurs without any identifiable motor symptoms, is abnormal and reflects subclinical alterations in brain function that accompany atherosclerotic occlusive vascular disease.

Enhanced ipsilateral motor activity has been seen previously during paralytic hand movement in patients with destructive lesions, such as occurring with brain tumor or after stroke, and was initially considered compensatory.[12,17] It has been proposed recently that this activity has a hyperactive component attributable, in some cases, to interhemispheric disinhibition.[18,19] Our results that show characteristic ipsilateral distribution of βERD during grasping with the contralesional hand, a significantly increased activity in the ipsilateral hemisphere without a decrease on the side of the vascular lesion, and a "normal" behavior in the tapping task indicate that hyperactivity on the ipsilateral hemisphere seen in patients with vascular lesions but without motor impairment is not compensatory. These same findings would argue against the possibility that the abnormal ipsilateral motor activity represents an involvement of symmetrical brain areas during the motor task and suggest that the phenomenon originates from other mechanisms.

Similarly to our results, Krakauer et al[20] using functional MRI observed abnormally increased ipsilateral activity during a contralesional hand movement in 6 patients with a unilateral ICA occlusion. The motor tasks they used had observation time windows of 20 seconds for the "active" and "control" states, comparable to those in the hand grasping of our study. However, when we analyzed with MEG during the self-paced tapping task (much shorter, 300-ms periods), we could not detect abnormal ipsilateral activity. This suggests that the different observation time windows record different brain activities.

During a voluntary hand motion, βERD is observed before and during movement execution and is followed by post-movement ERS.[7,21] These frequency changes distribute on the sensorimotor area bilaterally but primarily on the hemisphere contralateral to the examined hand.[7] The postmovement ERS is thought to reflect an inactive, "idling" state and shows an asymmetrical feature considered to be caused by a difference in handedness-related interhemispheric inhibition, "which is more prominent from the dominant than from the

nondominant hemisphere."[21,22] In our study, the "active" time window for hand-grasping was wide enough to encompass the whole of pre-, during-, and postmovement periods; however, that for the tapping task included premovement and motor execution, but less of the postmovement activity. If the postmovement ERS on the ipsilateral hemisphere, which is affected by the inhibition from the contralateral side, is decreased, then it would result in an increase of t value of ERD. Therefore, we propose that when 1 hemisphere activates, the impairment of its inhibitory function induces oscillatory change at the opposite side. For example, when during right hand-grasping in a patient with left ICA stenosis an impairment of the inhibitory function on the left hemisphere fails to deactivate the right hemisphere, this leads to a decrease of ERS on the right hemisphere, and we detect it as the ipsilateral dominant distribution of βERD. A statistically significant relation between the latter and the PVH in the AS group (Table 4) may indicate the contribution of the white matter damage to this phenomenon.

In the present work, we did not measure directly the postmovement ERS because of the difficulty in defining adequately the variation in time periods of post-tap finger movement and the influence of sensory input after the tap. Further studies using different tasks or other methods, such as transcranial magnetic stimulation, to measure cortical inhibitory function are required to confirm or refute our speculation. It should also be mentioned that measurements of motor activity that include pre- and postmovement time periods yield results for "activated areas" that might be strongly influenced by the inhibitory function of the primary activated hemisphere. It would be a great step forward if MEG could be used to evaluate brain activity of duration short enough to be less influenced by inhibitory functions.

Although the abnormal ipsilateral-dominant pattern was seen significantly more often in older patients and in those with higher scores for PVH and ventricular size, it is interesting that the clinically important indications for surgical intervention or stroke prevention, such as "impairment of vasoreactivity," "presence of symptoms," and "presence of an asymptomatic infarction," showed no significant relation. It can be suggested that in addition to CBF impairment caused by occlusive lesions in large vessels, some other factors related to aging and systemic atherosclerosis, which accompany morphological changes such as PVH, may induce subclinical alteration in motor-related cortical activity. A significantly higher incidence of abnormal ipsilateral pattern in patients with MCA lesions might indicate that it reflects functional alterations in particular in this vessel's territory.

In addition to stroke, atherosclerotic occlusive vascular diseases include slow but progressive pathological components that may induce atrophy or white matter change and result in functional impairments, such as vascular dementia. Detection with MEG of ipsilateral hyperactivity, an objective and quantitative measurement independent of CBF or metabolism, could greatly help in early diagnosis and treatment of functional alteration accompanying ischemic cerebrovascular disease.

Summary

We detected abnormal ipsilateral hyperactivity during a contralesional hand-grasping task in patients with atherosclerotic occlusive vascular disease. This phenomenon may represent an impairment of cortical inhibitory function caused by a vascular lesion. Evaluation with MEG could contribute to diagnosis and prevention of functional deteriorations that accompany this class of diseases.

Sources of Funding

This work was supported by grant-in-aid for scientific research (19790995) from the Japanese Ministry of Education, Science and Culture, by a grant from National Cardiovascular Research Institute (J040701213, J050701211), and by a grant from Public Health Research Foundation (Tokyo, Japan).

Disclosures

None.

References

1. North American Symptomatic Carotid Endarterectomy Trial Collaborators. Beneficial effect of carotid endarterectomy in symptomatic patients with high-grade carotid stenosis. *N Engl J Med*. 1991;325:445–453.
2. Kern R, Steinke W, Daffertshofer M, Prager R, Hennerici M. Stroke recurrences in patients with symptomatic vs asymptomatic middle cerebral artery disease. *Neurology*. 2005;65:859–864.
3. Mathiesen EB, Waterloo K, Joakimsen O, Bakke SJ, Jacobsen EA, Bonaa KH. Reduced neuropsychological test performance in asymptomatic carotid stenosis: The Tromso study. *Neurology*. 2004;62:695–701.
4. Chatrian GE, Petersen MC, Lazarte JA. The blocking of the rolandic wicket rhythm and some central changes related to movement. *Electroencephalogr Clin Neurophysiol*. 1959;11:497–510.
5. Pfurtscheller G. Graphical display and statistical evaluation of event-related desynchronization (ERD). *Electroencephalogr Clin Neurophysiol*. 1977;43:757–760.
6. Neuper C, Pfurtscheller G. Event-related dynamics of cortical rhythms: Frequency-specific features and functional correlates. *Int J Psychophysiol*. 2001;43:41–58.
7. Pfurtscheller G. Central beta rhythm during sensorimotor activities in man. *Electroencephalogr Clin Neurophysiol*. 1981;51:253–264.
8. Crone NE, Miglioretti DL, Gordon B, Lesser RP. Functional mapping of human sensorimotor cortex with electrocorticographic spectral analysis. Ii. Event-related synchronization in the gamma band. *Brain*. 1998;121:2301–2315.
9. Oshino S, Kato A, Wakayama A, Taniguchi M, Hirata M, Yoshimine T. Magnetoencephalographic analysis of cortical oscillatory activity in patients with brain tumors: Synthetic aperture magnetometry (SAM) functional imaging of delta band activity. *Neuroimage*. 2007;34:957–964.
10. Robinşon SE, Vrba J. Functional neuroimaging by synthetic aperture magnetometry (SAM). *Recent Advances in Biomagnetism*. Sendai, Tohoku University Press;1999:302–305.
11. Taniguchi M, Kato A, Fujita N, Hirata M, Tanaka H, Kihara T, Ninomiya H, Hirabuki N, Nakamura H, Robinson SE, Cheyne D, Yoshimine T. Movement-related desynchronization of the cerebral cortex studied with spatially filtered magnetoencephalography. *Neuroimage*. 2000;12:298–306.
12. Taniguchi M, Kato A, Ninomiya H, Hirata M, Cheyne D, Robinson SE, Maruno M, Saitoh Y, Kishima H, Yoshimine T. Cerebral motor control in patients with gliomas around the central sulcus studied with spatially filtered magnetoencephalography. *J Neurol Neurosurg Psychiatry*. 2004;75:466–471.
13. Hirata M, Kato A, Taniguchi M, Saitoh Y, Ninomiya H, Ihara A, Kishima H, Oshino S, Baba T, Yorifuji S, Yoshimine T. Determination of language dominance with synthetic aperture magnetometry: Comparison with the Wada test. *Neuroimage*. 2004;23:46–53.

14. Oldfield RC. The assessment and analysis of handedness: The Edinburgh inventory. *Neuropsychologia*. 1971;9:97–113.
15. Manolio TA, Kronmal RA, Burke GL, Poirier V, O'Leary DH, Gardin JM, Fried LP, Steinberg EP, Bryan RN. Magnetic resonance abnormalities and cardiovascular disease in older adults. The cardiovascular health study. *Stroke*. 1994;25:318–327.
16. Imaizumi M, Kitagawa K, Hashikawa K, Oku N, Teratani T, Takasawa M, Yoshikawa T, Rishu P, Ohtsuki T, Hori M, Matsumoto M, Nishimura T. Detection of misery perfusion with split-dose ^{123}I-iodoamphetamine single-photon emission computed tomography in patients with carotid occlusive diseases. *Stroke*. 2002;33:2217–2223.
17. Johansen-Berg H, Rushworth MF, Bogdanovic MD, Kischka U, Wimalaratna S, Matthews PM. The role of ipsilateral premotor cortex in hand movement after stroke. *Proc Natl Acad Sci U S A*. 2002;99:14518–14523.
18. Shimizu T, Hosaki A, Hino T, Sato M, Komori T, Hirai S, Rossini PM. Motor cortical disinhibition in the unaffected hemisphere after unilateral cortical stroke. *Brain*. 2002;125:1896–1907.
19. Murase N, Duque J, Mazzocchio R, Cohen LG. Influence of interhemispheric interactions on motor function in chronic stroke. *Ann Neurol*. 2004;55:400–409.
20. Krakauer JW, Radoeva PD, Zarahn E, Wydra J, Lazar RM, Hirsch J, Marshall RS. Hypoperfusion without stroke alters motor activation in the opposite hemisphere. *Ann Neurol*. 2004;56:796–802.
21. Pfurtscheller G, Stancak A Jr, Neuper C. Post-movement beta synchronization. A correlate of an idling motor area? *Electroencephalogr Clin Neurophysiol*. 1996;98:281–293.
22. Stancak A Jr, Pfurtscheller G. Event-related desynchronisation of central beta-rhythms during brisk and slow self-paced finger movements of dominant and nondominant hand. *Brain Res Cogn Brain Res*. 1996;4:171–183.

J Neurosurg 107:555–559, 2007

Reduction of intractable deafferentation pain due to spinal cord or peripheral lesion by high-frequency repetitive transcranial magnetic stimulation of the primary motor cortex

YOUICHI SAITOH, M.D., PH.D.,[1] AZUMA HIRAYAMA, M.D.,[1] HARUHIKO KISHIMA, M.D., PH.D.,[1] TOSHIO SHIMOKAWA, PH.D.,[2] SATORU OSHINO, M.D., PH.D.,[1] MASAYUKI HIRATA, M.D., PH.D.,[1] NAOKI TANI, M.D.,[1] AMAMI KATO, M.D., PH.D.,[1] AND TOSHIKI YOSHIMINE, M.D., PH.D.[1]

[1]Department of Neurosurgery, Osaka University Graduate School of Medicine; and [2]Graduate School of Medicine and Engineering, University of Yamanashi, and Medical Center for Translational Research, Osaka University Hospital, Osaka, Japan

Object. The authors previously reported that navigation-guided repetitive transcranial magnetic stimulation (rTMS) of the precentral gyrus relieves deafferentation pain. Stimulation parameters were 10 trains of 10-second 5-Hz TMS pulses at 50-second intervals. In the present study, they used various stimulation frequencies and compared efficacies between two types of lesions.

Methods. Patients were divided into two groups: those with a cerebral lesion and those with a noncerebral lesion. The rTMS was applied to all the patients at frequencies of 1, 5, and 10 Hz and as a sham procedure in random order. The effect of rTMS on pain was rated by patients using a visual analog scale.

Results. The rTMS at frequencies of 5 and 10 Hz, compared with sham stimulation, significantly reduced pain, and the pain reduction continued for 180 minutes. A stimulation frequency of 10 Hz may be more effective than 5 Hz, and at 1 Hz was ineffective. The effect of rTMS at frequencies of 5 and 10 Hz was greater in patients with a noncerebral lesion than those with a cerebral lesion.

Conclusions. High-frequency (5- or 10-Hz) rTMS of the precentral gyrus can reduce intractable deafferentation pain, but low-frequency stimulation (at 1 Hz) cannot. Patients with a noncerebral lesion are more suitable candidates for high-frequency rTMS of the precentral gyrus. *(DOI: 10.3171/JNS-07/09/0555)*

KEY WORDS • deafferentation pain • imaging-guided navigation • motor cortex • repetitive transcranial magnetic stimulation

DEAFFERENTATION or neuropathic pain caused by a cerebral, spinal cord, or peripheral lesion is one of the most difficult types of pain to treat, and most cases are refractory to medical treatment. Only MCS has been shown to provide relief in cases of such deafferentation pain, and relief is achieved in only 50 to 70% of patients.[4,9,11,18] The mechanism underlying the effects of MCS in reducing pain remains controversial. However, the precentral gyrus is a common target for cortical stimulation in the treatment of medically intractable deafferentation pain.[1,4,9,11,14,16–18] According to recent reports,[3,7,8,13,21,22] rTMS of the precentral gyrus provides an effect similar to that of MCS in patients with medically intractable deafferentation pain. However, it can be difficult to stimulate the same cortical area repeatedly, and results tend to vary. In addition, the electric current evoked by rTMS is generally confined to the cortex.[19] For these reasons, we have used navigation-guided rTMS in patients with intractable deafferentation pain to precisely stimulate specific cerebral cortical areas.

We have previously reported that navigation-guided 5-Hz rTMS of the precentral gyrus significantly reduced intractable neuropathic pain in 50% of patients.[2] We selected four cortical targets for navigation-guided rTMS: the precentral gyrus, the postcentral gyrus, the premotor cortex, and the supplementary motor area. However, only stimulation of the precentral gyrus produced pain relief. In addition to the cortical target for rTMS, the stimulation parameters and the type of lesion are important. In the present study, we varied the stimulation frequency for navigation-guided rTMS of the precentral gyrus and compared the efficacies of the various frequencies, particularly between origins of pain.

Abbreviations used in this paper: ANOVA = analysis of variance; MCS = motor cortex stimulation; rTMS = repetitive transcranial magnetic stimulation; SF-MPQ = short-form McGill Pain Questionnaire; VAS = visual analog scale.

Clinical Material and Methods

Patient Population

The patient population comprised 13 right-handed patients (seven men and six women; age range 29–76 years,

mean age 59.4 years) suffering from intractable deafferentation pain. Seven of the patients were suffering from poststroke pain due to thalamic hemorrhage or infarction (three), or putaminal hemorrhage (four). Two patients were suffering from deafferentation pain originating from a spinal cord lesion (ruptured arteriovenous malformation or infarction), and one patient each was suffering from pain due to brachial plexus injury, peripheral nerve injury, a cauda equina lesion, or a phantom limb. Patient characteristics are listed in Table 1. Patients were assigned to one of two groups according to the type of lesion: cerebral lesion, or spinal cord or peripheral lesion (noncerebral lesion). Patients were given anticonvulsants, nonsteroidal anti-inflammatory drugs, and antidepressants, as needed and also during the rTMS sessions. Patients also underwent psychological examination and electroencephalographic examination before rTMS to assess whether seizure development was likely. Patients who experienced pain reduction in response to 5-Hz stimulation were enrolled in this study. Informed consent was obtained from all study participants. The study was approved by the Ethics Committee of Osaka University Hospital, and all patients were blinded to the area being stimulated and to the expected effect.

TABLE 1

*Characteristics of patients experiencing intractable deafferentation pain**

Case No.†	Age (yrs), Sex	Diagnosis	Pain	
			Duration (yrs)	Location
1	59, M	rt putaminal hemorrhage	16	lt lower limb
2	57, F	lt putaminal hemorrhage	5	rt lower limb
3	62, M	lt thalamic hemorrhage	8.5	rt upper limb
4	70, M	lt thalamic infarction	2.2	rt upper limb
5	64, F	lt putaminal hemorrhage	6.9	rt lower limb
6	74, F	lt putaminal hemorrhage	35	rt lower limb
7	76, F	lt thalamic infarction	2	rt upper limb
8	55, F	spinal cord infarction	2.6	lt lower limb
9	29, M	ruptured spinal AVM	5.5	rt lower limb
10	62, M	phantom limb pain	7	bilat lower limbs
11	41, M	cauda equina lesion	6.3	rt lower limb
12	72, M	lt brachial plexus injury	11	lt upper limb
13	51, F	peripheral nerve injury	24.3	lt lower limb

* AVM = arteriovenous malformation.

† The patients in Cases 1 to 7 experienced neuropathic pain due to a cerebral lesion, and those in Cases 8 to 13 had neuropathic pain due to a spinal cord or peripheral lesion.

The rTMS Procedure

The rTMS was applied through a figure-eight coil (MC B-70, Medtronic Functional Diagnostics A/S), which provides limited cortical stimulation. The coil was connected to a MagPro magnetic stimulator (Medtronic Functional Diagnostics A/S). The resting motor threshold of the affected muscle area was determined by stimulation of the corresponding precentral gyrus area and electromyography in the affected area. The resting motor threshold at 90% intensity was used for treatment. Muscle twitches can be elicited in painful areas, if stimulated carefully according to somatotopy. This is possible even with trigeminal lesions and in the lower limbs. For patients in whom muscle twitches in painful areas were difficult to elicit due to severe damage of motor pathways, rTMS was applied with an intensity of 100 A/μsec. This was the maximum tolerable intensity for most patients in our study, with higher intensities resulting in scalp pain.[2] A potential equivalent to 90% of the intensity of the resting motor threshold was used for treatment. Ten trains of 10-second 5-Hz TMS pulses with 50-second intervals between trains, five trains of 10-second 10-Hz TMS pulses with 50-second intervals between trains, continuous 1-Hz TMS pulses for 500 seconds, and sham 5-Hz TMS pulses were applied to the precentral gyrus in random order. A total of 500 stimulations were applied for each parameter, and there was an interval of about 48 hours before each new series of stimulations was performed. Sham stimulation was applied as described previously.[2,21] In brief, the parameters were the same as for actual stimulations, but the coil was placed at a 45° angle to the skull, and synchronized electrical stimulations were delivered to the forehead. The protocol was in compliance with the Guidelines for the Safe Use of rTMS.[23] The TMS coil was held and positioned by an articulated coil holder. The Brainsight Frameless navigation system (Rogue Research Inc.) was used to monitor the position and direction of the coil and the position of the patient's head, as described previously.[2]

Evaluation of Pain Relief

Using a VAS and the SF-MPQ, the patients evaluated their own pain before and after (at 0, 15, 30, 60, 90, and 180 minutes) rTMS (at 1, 5, and 10 Hz) or sham stimulation.

Statistical Analysis

We evaluated the effectiveness of stimulation for each patient according to the reduction rate of VAS scores (reduction rate = $1 - VAS_{poststimulation}/VAS_{prestimulation}$). We evaluated the influence of the various frequencies (sham, and 1, 5, and 10 Hz) and lesion types by applying repeated-measures ANOVA to the reduction rate of VAS. To compare sham stimulation with rTMS (at 1, 5, and 10 Hz), we used the Dunnett multiple-comparisons at various points after stimulation (Fig. 1).

Results

All 13 patients participated in all planned sessions of navigation-guided rTMS, and no transient or lasting side effects, including convulsion, were observed. Patients were unable to distinguish sham stimulation from rTMS because the synchronized electrical stimulation applied to the forehead induced forehead spasms. All 13 patients underwent sham stimulation and 1-, 5-, and 10-Hz rTMS of the precentral gyrus. Repeated-measures ANOVA indicated that the frequency of stimulation ($p = 0.03$) and the presence or absence of a cerebral lesion ($p = 0.04$) contributed to pain reduction as judged by the reduction rate of VAS scores. Interaction between these factors was not significant ($p = 0.80$). The reduction rates of VAS scores for each frequency are shown in Fig. 1. Stimulations at 5 and 10 Hz, compared with sham stimulation, were effective in reducing pain for up to 180 minutes ($p < 0.05$, repeated-measures ANOVA). Stimulation at 1 Hz did not differ from sham stimulation. In the cerebral lesion group, 5- and 10-Hz

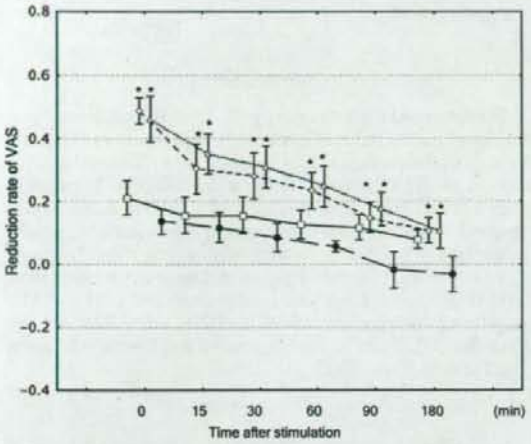

FIG. 1. Graph showing the reduction rate of VAS in all 13 patients after sham stimulation and 1-, 5- and 10-Hz rTMS of the precentral gyrus. As a result of repeated-measures ANOVA, the frequency of stimulation and the presence or absence of a cerebral lesion contributed to pain reduction as determined by a decrease in the VAS. Patients exhibited significant pain reduction after 5- and 10-Hz rTMS (but not after 1-Hz rTMS) compared with sham stimulation until 180 minutes, as indicated by the VAS scores. The VAS scores are presented as the means ± standard error of the means (SEMs). *$p < 0.05$. *Circles* denote sham stimulation; *squares*, 1-Hz rTMS; *diamonds*, 5-Hz rTMS; and *triangles*, 10-Hz rTMS.

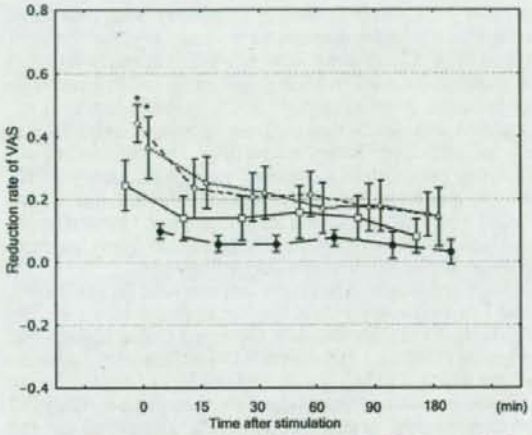

FIG. 2. Graph showing the reduction rate in VAS scores in the cerebral lesion group (seven patients). According to the Dunnett multiple-comparisons procedure, rTMS at 5 and 10 Hz, compared with sham stimulation, significantly reduced pain as determined by the reduction rate of VAS score only just after rTMS. The VAS scores are presented as the means ± SEMs. *$p < 0.05$.

rTMS, in comparison to sham stimulation, resulted in significant pain reduction just after rTMS ($p < 0.05$, according to Dunnett multiple-comparisons), and the mean reduction in VAS scores just after rTMS was greater than 30% (Fig. 2). In the noncerebral lesion group, 5- Hz rTMS resulted in significant pain reduction at 0, 30, and 90 minutes after rTMS ($p < 0.05$), and the mean reduction in VAS scores was greater than 30% for up to 30 minutes. The rTMS at 10 Hz, compared with sham stimulation, resulted in significant pain reduction for up to 90 minutes ($p < 0.05$), and the mean reduction in VAS scores was greater than 30% for up to 60 minutes (Fig. 3). The rTMS did not produce a consistent change in SF-MPQ scores. In patients with a high baseline SF-MPQ score (> 20), the VAS and SF-MPQ scores tended to be similar. In patients with a low baseline SF-MPQ score (< 10), the SF-MPQ score changed little, regardless of a reduction in the VAS score.

Discussion

In our previous study,[2] only 5-Hz rTMS of the precentral gyrus, compared with rTMS of adjacent cortical areas (the postcentral gyrus, the premotor cortex, and the supplementary motor area), relieved pain. Appropriate stimulation parameters (for example, stimulation frequency) have remained uncertain. In the present study, 5- and 10-Hz rTMS of the precentral gyrus were significantly more effective than sham stimulation, but 1-Hz rTMS was not. The rTMS may be more effective at 10 Hz than at 5 Hz (Figs. 1–3). Correlation between the efficacy of rTMS and type of lesion was also investigated. Deafferentation pain caused by a cerebral lesion was more refractory to rTMS than that caused by a spinal cord or peripheral lesion (Figs. 2 and 3).

Pain reduction in response to rTMS of the precentral gyrus was likely due to modification of pain perception, as previously reported.[3,13] The detailed mechanism underlying pain relief in response to MCS was examined by positron emission tomography activation studies.[1,17] The MCS ap-

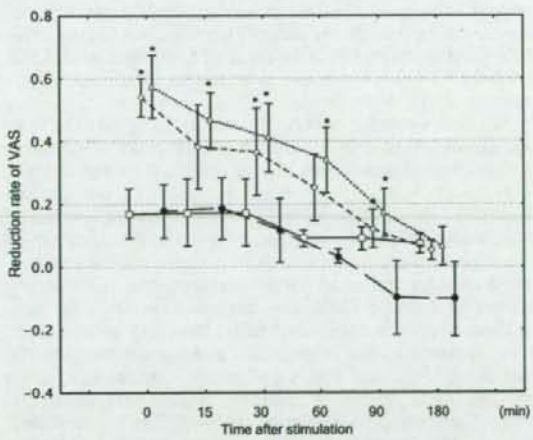

FIG. 3. Graph showing the reduction rate of VAS scores in the noncerebral lesion group (six patients). According to the Dunnett multiple-comparisons procedure, rTMS at 5 Hz significantly reduced pain as determined by the decrease in VAS score at 0, 30, and 90 minutes; rTMS at 10 Hz significantly reduced pain for up to 90 minutes. The reduction rate of the VAS score for 10 Hz was greater than that for 5 Hz at each time point after stimulation. The VAS scores are presented as the means ± SEMs. *$p < 0.05$.

pears to activate several brain areas involved in pain perception.[1,17] A common finding in patients with poststroke pain was a relative decrease in thalamic regional cerebral blood flow during chronic pain.[12] We previously reported activation of the anterior cingulate gyrus and left posterior thalamus in response to right MCS.[17] Garcia-Larrea et al.[1] reported that MCS may activate cingulate, orbitofrontal cortex, and upper brainstem regions. The mechanism underlying pain relief in response to high-frequency rTMS may be similar to that of MCS.[5] Several brain regions associated with pain perception may be activated by subthreshold high-frequency rTMS of the precentral gyrus and may reduce deafferentation pain comprehensively.

High-frequency rTMS enhances neuronal firing efficacy, and low-frequency rTMS has the opposite effect.[6,20] The rTMS at 20 Hz significantly increased global blood flow, whereas rTMS at 1 Hz did not.[20] Lefaucheur et al.[7] evaluated the effect of rTMS at two frequencies (10 and 0.5 Hz) in 18 patients with intractable unilateral hand pain. The VAS score improved in response to 10-Hz stimulation but did not improve in response to 0.5-Hz stimulation. In addition, good pain control has been reported in response to high-frequency stimulation (10 or 20 Hz) in some rTMS studies.[13,22] Effectiveness of low-frequency (1-Hz) rTMS was reported only in healthy individuals with acute pain caused by capsaicin.[21] The findings are consistent with our results indicating that 5- and 10-Hz rTMS are effective but 1-Hz rTMS is not.

It is likely that the greater the stimulation frequency, the greater the effect of rTMS on pain reduction. Lefaucheur et al.[8] used 80% of the resting motor threshold of the intact hand for rTMS treatment of deafferentation pain. We used 90% of the resting motor threshold of the affected limb, and our rTMS was of higher power than theirs. Our success rate seemed to be superior to theirs. However, suprathreshold rTMS of the precentral gyrus corresponding to the affected limb and stimulation at frequencies of greater than 10 Hz appear to increase the risk of seizure development in patients who have suffered stroke. Therefore, we did not evaluate these types of rTMS. In the future, subthreshold rTMS with 5 or 10 Hz may prove to be useful for clinical applications of rTMS.

We believe that it is very difficult to apply all rTMSs to the same cortical area. We therefore performed rTMS using a frameless magnetic resonance imaging–guided navigation system in accordance with each patient's own cortical anatomy. The TMS coil was positioned by an articulated coil holder. Without a navigation system, identification of the precentral gyrus is difficult in patients with severe motor weakness whose motor evoked response is barely induced by a single TMS. The anatomical error of the navigation system is considered to be less than about 5 mm. This is based on the observation that muscle twitches did not occur if the coil was out of position by about 1 cm on the magnetic resonance imaging–guided navigation system. Experimental simulation showed that the electrical current induced with the figure-eight coil is considerably limited in the cortex. We consider a navigation system to be indispensable when performing rTMS.

We have reported that there is good correlation between the results of rTMS and those of MCS.[15] Migita et al.[10] reported on two patients with central pain who were evaluated using rTMS of precentral gyrus and then treated using MCS. We believe that high-frequency rTMS can predict the results of MCS.

Conclusions

Subthreshold high-frequency rTMS of the precentral gyrus significantly reduces intractable pain for up to 180 minutes. Low-frequency rTMS is ineffective. Treatment with the aid of rTMS appears to be more effective in patients with a spinal cord or peripheral lesion than in those with a cerebral lesion. Several brain regions associated with pain perception may be activated by subthreshold high-frequency rTMS of the precentral gyrus, and such stimulation may reduce deafferentation pain comprehensively. The rTMS may be a good predictor of MCS efficacy, and thus, we believe that MCS can be recommended to patients who have good results from rTMS.

References

1. Garcia-Larrea L, Peyron R, Mertens P, Gregoire MC, Lavenne F, Le Bars D, et al: Electrical stimulation of motor cortex for pain control: a combined PET-scan and electrophysiological study. **Pain 83:**259–273, 1999
2. Hirayama A, Saitoh Y, Kishima H, Shimokawa T, Oshino S, Hirata M, et al: Reduction of intractable deafferentation pain by navigation-guided repetitive transcranial magnetic stimulation (rTMS) of the primary motor cortex. **Pain 122:**22–27, 2006
3. Kanda M, Mima T, Oga T, Matsuhashi M, Toma K, Hara H, et al: Transcranial magnetic stimulation (TMS) of the sensorimotor cortex and medial frontal cortex modifies human pain perception. **Clin Neurophysiol 114:**860–866, 2003
4. Katayama Y, Fukaya C, Yamamoto T: Poststroke pain control by chronic motor cortex stimulation. Neurological characteristics predicting a favorable response. **J Neurosurg 89:**585–591, 1998
5. Kimbrell TA, Dunn RT, George MS, Danielson AL, Willis MW, Repella JD, et al: Left frontal-repetitive transcranial magnetic stimulation (rTMS) and regional cerebral glucose metabolism in normal volunteers. **Psychiatry Res 115:**101–113, 2002
6. Kimbrell TA, Little JT, Dunn RT, Frye MA, Greenberg BD, Wassermann EM, et al: Frequency dependence of antidepressant response to left prefrontal repetitive transcranial magnetic stimulation (rTMS) as a function of baseline cerebral glucose metabolism. **Biol Psychiatry 46:**1603–1613, 1999
7. Lefaucheur JP, Drouot X, Keravel Y, Nguyen JP: Pain relief induced by repetitive transcranial magnetic stimulation of precentral cortex. **Neuroreport 12:**2963–2965, 2001
8. Lefaucheur JP, Drouot X, Menard-Lefaucheur I, Zerah F, Bendib B, Cesaro P, et al: Neurogenic pain relief by repetitive transcranial magnetic cortical stimulation depends on the origin and the site of pain. **J Neurol Neurosurg Psychiatry 75:**612–616, 2004
9. Meyerson BA, Lindblom U, Linderoth B, Lind G, Herregodts P: Motor cortex stimulation as treatment of trigeminal neuropathic pain. **Acta Neurochir Suppl (Wien) 58:**150–153, 1993
10. Migita K, Uozumi T, Arita K, Monden S: Transcranial magnetic coil stimulation of motor cortex in patients with central pain. **Neurosurgery 36:**1039–1040, 1995
11. Nguyen JP, Keravel Y, Feve A, Uchiyama T, Cesaro P, Le Guerinel C, et al: Treatment of deafferentation pain by chronic stimulation of the motor cortex: report of a series of 20 cases. **Acta Neurochir Suppl 68:**54–60, 1997
12. Peyron R, Garcia-Larrea L, Deiber MP, Cinotti L, Convers P, Sindou M, et al: Electrical stimulation of precentral cortical area in the treatment of central pain: electrophysiological and PET study. **Pain 62:**275–286, 1995
13. Pleger B, Janssen F, Schwenkreis P, Volker B, Maier C, Tegent-

hoff M: Repetitive transcranial magnetic stimulation of the motor cortex attenuates pain perception in complex regional pain syndrome type I. **Neurosci Lett 356:**87–90, 2004
14. Rainov NG, Heidecke V: Motor cortex stimulation for neuropathic facial pain. **Neurol Res 25:**157–161, 2003
15. Saitoh Y, Hirayama A, Kishima H, Oshino S, Hirata M, Kato A, et al: Stimulation of primary motor cortex for intractable deafferentation pain. **Acta Neurochir Suppl 99:**57–59, 2006
16. Saitoh Y, Kato A, Ninomiya H, Baba T, Shibata M, Mashimo T, et al: Primary motor cortex stimulation within the central sulcus for treating deafferentation pain. **Acta Neurochir Suppl 87:** 149–152, 2003
17. Saitoh Y, Osaki Y, Nishimura H, Hirano S, Kato A, Hashikawa K, et al: Increased regional cerebral blood flow in the contralateral thalamus after successful motor cortex stimulation in a patient with poststroke pain. **J Neurosurg 100:**935–939, 2004
18. Saitoh Y, Shibata M, Hirano S, Hirata M, Mashimo T, Yoshimine T: Motor cortex stimulation for central and peripheral deafferentation pain. **J Neurosurg 92:**150–155, 2000
19. Sekino M, Ueno S: FEM-based determination of optimum current distribution in transcranial magnetic stimulation as an alternative to electroconvulsive therapy. **IEEE Trans Magn 40:**2167–2169, 2004
20. Speer AM, Kimbrell TA, Wassermann EM, Repella JD, Willis MW, Herscovitch P, et al: Opposite effects of high and low frequency rTMS on regional brain activity in depressed patients. **Biol Psychiatry 48:**1133–1141, 2000
21. Tamura Y, Okabe S, Ohnishi T, Saito DN, Arai N, Mochio S, et al: Effects of 1-hz repetitive transcranial magnetic stimulation on acute pain induced by capsaicin. **Pain 107:**107–115, 2004
22. Topper R, Foltys H, Meister IG, Sparing R, Boroojerdi B: Repetitive transcranial magnetic stimulation of the parietal cortex transiently ameliorates phantom limb pain-like syndrome. **Clin Neurophysiol 114:**1521–1530, 2003
23. Wassermann EM: Risk and safety of repetitive transcranial magnetic stimulation: report and suggested guidelines from the International Workshop on the Safety of Repetitive Transcranial Magnetic Stimulation, June 5–7, 1996. **Electroencephalogr Clin Neurophysiol 108:**1–16, 1998

Manuscript submitted July 25, 2006.
Accepted September 20, 2006.
Address reprint requests to: Youichi Saitoh, M.D., Ph.D., Department of Neurosurgery, Osaka University Graduate School, 2-2 Yamadaoka, Suita-shi, Osaka, 565-0871, Japan. neurosaitoh@mbk.nifty.com.

J Neurosurg 107:43–48, 2007

Motor cortex stimulation in patients with deafferentation pain: activation of the posterior insula and thalamus

HARUHIKO KISHIMA, M.D., PH.D.,[1] YOUICHI SAITOH, M.D., PH.D.,[1] YASUHIRO OSAKI, M.D., PH.D.,[2,3] HIROSHI NISHIMURA, M.D., PH.D.,[3] AMAMI KATO, M.D., PH.D.,[1] JUN HATAZAWA, M.D., PH.D.,[2] AND TOSHIKI YOSHIMINE, M.D., PH.D.[1]

Departments of [1]Neurosurgery, [2]Tracer Kinetics, and [3]Otorhinolaryngology, Osaka University Medical School, Suita, Osaka, Japan

Object. The mechanisms underlying deafferentation pain are not well understood. Motor cortex stimulation (MCS) is useful in the treatment of this kind of chronic pain, but the detailed mechanisms underlying its effects are unknown.

Methods. Six patients with intractable deafferentation pain in the left hand were included in this study. All were right-handed and had a subdural electrode placed over the right precentral gyrus. The pain was associated with brainstem injury in one patient, cervical spine injury in one patient, thalamic hemorrhage in one patient, and brachial plexus avulsion in three patients. Treatment with MCS reduced pain; visual analog scale (VAS) values for pain were 82 ± 20 before MCS and 39 ± 20 after MCS (mean ± standard error). Regional cerebral blood flow (rCBF) was measured by positron emission tomography with $H_2{}^{15}O$ before and after MCS. The obtained images were analyzed with statistical parametric mapping software (SPM99).

Results. Significant rCBF increases were identified after MCS in the left posterior thalamus and left insula. In the early post-MCS phase, the left posterior insula and right orbitofrontal cortex showed significant rCBF increases, and the right precentral gyrus showed an rCBF decrease. In the late post-MCS phase, a significant rCBF increase was detected in the left caudal part of the anterior cingulate cortex (ACC).

Conclusions. These results suggest that MCS modulates the pathways from the posterior insula and orbitofrontal cortex to the posterior thalamus to upregulate the pain threshold and pathways from the posterior insula to the caudal ACC to control emotional perception. This modulation results in decreased VAS scores for deafferentation pain.
(DOI: 10.3171/JNS-07/07/0043)

KEY WORDS • **deafferentation pain** • **motor cortex stimulation** • **posterior insula** • **posterior thalamus** • **regional cerebral blood flow**

DEAFFERENTATION pain is the most difficult type of pain to treat. Tsubokawa et al.[38] developed the use of MCS. Katayama et al.[14] reported that the use of MCS provided pain relief in approximately 50% of patients with thalamic pain. Meyerson[19] and Nguyen[21,22] and their colleagues showed that facial deafferentation pain was decreased by MCS. Son et al.[34] reported the effectiveness of MCS on complex regional pain syndrome Type II. We also reported that MCS is effective for treating peripheral and spinal cord deafferentation pain (brachial plexus injuries, phantom limb pain, and spinal cord injuries).[30]

Recent advances in functional imaging and neurophysiological methods have made it possible to examine neuronal activity in response to various tasks. Cerebral responses to peripheral pain have also been studied by many investigators in animal models of acute pain and in normal volunteers undergoing thermal, laser, or chemical stimulation.[12,17,18,20,24,33,42] Because animal models of chronic pain are difficult to carry out, few studies have focused on the mechanisms of chronic intractable pain,[28] although authors have speculated on the mechanisms on the basis of clinical results. The mechanism of MCS in the treatment of post-stroke pain was addressed by Tsubokawa et al.[39] They speculated that fourth-order nonnociceptive neurons are activated by MCS and inhibit hyperactive nociceptive neurons. It has also been reported that the anterior thalamus, brainstem, cingulate gyrus, and orbitofrontal cortex are activated during MCS.[10,25] The somatosensory cortex is not activated by MCS. Motor cortex stimulation may influence the affective-emotional component of chronic pain, and inhibitory control of pain involves thalamic and brainstem relays to descending pathways down to spinal cord segments, resulting in the attenuation of spinal flexion reflexes. The results of our preliminary PET study showed that the contralateral posterior thalamus was activated after treatment with right MCS for thalamic pain.[29]

Abbreviations used in this paper: ACC = anterior cingulate cortex; BA = Brodmann area; ICBM = International Consortium for Brain Mapping; FWHM = full width at half maximum; MCS = motor cortex stimulation; M1 = primary motor cortex; PET = positron emission tomography; rCBF = regional cerebral blood flow; SPM = statistical parametric mapping; VAS = visual analog scale.

In the present study, we used $H_2{}^{15}O$ PET to investigate the pattern of MCS-related neuronal activation and/or attenuation before and after MCS; $H_2{}^{15}O$ PET shows rCBF, which reflects focal neuronal activation.[13] We also used a recently developed method of statistical analysis involving parametric mapping of normalized brain images. Six patients with chronic deafferentation pain in the left hand and with electrodes placed on the right precentral gyrus corresponding to the M1 of the left hand were studied. This method provides more accurate results than those reported previously because the M1 is precisely and specifically stimulated.

Clinical Material and Methods

Patients and Surgical Procedure

Six right-handed patients (four men and two women, age range 50–67 years) with intractable deafferentation pain in the left hand were included in this study (Table 1). Deafferentation pain had resulted from brainstem injury (one patient), cervical spine injury (one patient), thalamic hemorrhage (one patient), and brachial plexus avulsion (three patients). The patients had suffered from intractable pain for 3 to 27 years, and medication had been ineffective. All of the patients showed slight to moderate motor weakness in the left arm. The VAS (grading range 0–100) and the short form of the McGill Pain Questionnaire were used to evaluate the degree of pain.

The surgical procedure was performed as described previously.[29,30] In brief, the location of the central sulcus was approximated with the use of preoperative magnetic resonance images and confirmed by intraoperative phase reverse of the N20 component of the somatosensory evoked potential upon stimulation of the left median nerve,[43] recorded with an evoked potential recorder (Neuropack 8, Nihon Kohden Co. Ltd.). A 20-grid set of electrodes (4 × 5 array, 0.3-cm-diameter electrode, 0.7-cm separation; Unique Medical Co. Ltd.) was implanted subdurally, covering the convexities of the pre- and postcentral gyri of the left hemisphere. After confirmation of pain reduction in response to stimulation for 10 to 14 days, a permanent four-array stimulating electrode (Resume II, model 3587A, Medtronic, Inc.) was placed subdurally at the surface of the right precentral gyrus at the site associated with the most effective pain reduction. The electrode was controlled by a subcutaneously implanted stimulator (Itrel III, Medtronic, Inc.).

Bipolar stimulation[30] was used for pain relief, and stimulation parameters varied in each patient. The general ranges were: voltage, 0.6 to 3.5 V; frequency, 25 to 40 Hz. The pulse width was 210 microseconds, and stimulation was administered for 30 minutes one to four times a day. The patients used MCS for at least 6 months.

The PET Scanning Procedure and Activation Task

The PET study was performed 1 to 3 years after implantation of the stimulation electrode. A Headtome V PET scanner (Shimadzu Co.) was used to scan in the 3D acquisition mode with a head shield. Patients went without cortical stimulation for more than 12 hours before the PET study. The patients lay with eyes closed in a silent and dim room. A 15-minute transmission scan was performed first with ^{68}Ge sources to correct for γ-ray attenuation. Relative cerebral blood flow was measured based on the distribution of radioactivity after slow bolus intravenous injection of $H_2{}^{15}O$ (7 mCi/scan, each lasting 90 seconds). Six PET scans corresponding to six $H_2{}^{15}O$ injections were performed before MCS; MCS was performed for approximately 30 minutes; and six PET scans were performed after confirmation of pain reduction. The PET protocol was as described previously.[29]

TABLE 1

General characteristics of patients with deafferentation pain

Case No.	Age (yrs), Sex	Associated Lesion	Duration of Pain (yrs)
1	50, F	brainstem injury	3.3
2	50, F	cervical spine injury	6.0
3	59, M	thalamic hemorrhage	8.3
4	67, M	brachial plexus avulsion	27.0
5	57, M	brachial plexus avulsion	4.0
6	56, M	brachial plexus avulsion	3.0

Data Analysis

Attenuation-corrected data were reconstructed into an image (voxel sizes: 2 × 2 × 3.125 mm; field of view: 256 × 256 × 196 mm) with a resulting resolution of 4 × 4 × 5 mm at FWHM. The images were analyzed with SPM software (SPM99; Wellcome Department of Cognitive Neurology).[7] The PET images were anatomically normalized in fit with ICBM coordinates of the Montreal Neurological Institute. Images from each patient were realigned to the first volume of PET images and normalized to the template[7] to account for variation in gyral anatomy and interindividual variability in structure–function relationships, and to improve the signal-to-noise ratio. This procedure was used for image realignment, anatomical normalization, smoothing (12 mm at FWHM), and statistical analysis.[15] Data were normalized to global blood flow (average 50). The effect of state-dependent differences in global blood flow was tested with analysis of covariance.

All six patients were included in the same statistical analyses, with voxel-to-voxel comparison. Statistical parametric maps were generated with an analysis of variance model using the General Linear Model formulation of SPM99.[9] We analyzed the main effect of MCS by comparing images obtained after MCS with those obtained before MCS with the statistical threshold set at a probability value of less than 0.005 for peak height, corrected for spatial extent (> eight voxels per cluster). We also categorized post-MCS sessions as follows: the first two scans in the 20 minutes just after MCS were denoted as the early post-MCS phase and the last two scans more than 40 minutes after MCS were denoted as the late post-MCS phase. We generated SPM (t) maps of rCBF changes associated with each comparison. For between-group comparisons, the SPM (t) maps were transformed into SPM (Z) maps, and the levels of significance of areas of activation were assessed according to peak height of foci estimation based on the theory of random Gaussian fields. Significance was accepted if a cluster showed a corrected probability value of less than 0.05. Data are presented as means ± standard errors.

This study adhered to the guidelines of the Declaration of Helsinki on the use of human subjects in research, and the patients provided written informed consent.

Results

Pain Reduction in Response to MCS

After MCS, all six patients showed various degrees of pain reduction according to VAS data (from a mean of 82 ± 20 to a mean of 39 ± 20). The duration of the MCS effect differed between the patients, ranging from 2 to 12 hours. In this study, we found that the pain reduction began during MCS and continued for at least 30 minutes after MCS. The pain reduction was stable during the six post-MCS PET scans. The results of the short form of the McGill Pain Questionnaire agreed for the most part with the VAS scores.

Brain Activation Profiles in Response to MCS

Comparison of rCBF before and after MCS showed significant rCBF increases after MCS in the left posterior thalamus (pulvinar) and left posterior insula (the six cases were analyzed together, corrected cluster $p = 0.044$; Table 2, Fig. 1A and B). No areas of significant rCBF decrease were identified. When we compared the scans obtained in the early post-MCS phase with the six pre-MCS scans, we found significant rCBF increases in the left posterior insula ($p = 0.011$) and the right orbitofrontal cortex (BA 11) ($p = 0.047$) (Table 2, Fig. 1C and D). Significant decreases in rCBF were identified between the right middle frontal gyrus (BA 9) and the right precentral gyrus (BA 4) ($p = 0.048$) (Table 3, Fig. 2).

When scans obtained in the late post-MCS phase were compared with the six pre-MCS scans, the left caudal part of the ACC (BA 24) showed significant increases in rCBF ($p = 0.005$; Table 2, Fig. 1E). Comparing rCBF in the early post-MCS phase with that in the late post-MCS phase, rCBF in the left medial frontal gyrus (supplementary motor area; BA 6) was increased in the late phase ($p = 0.033$, cluster size, 309; Talairach coordinates, $x = 3$, $y = -5$, $z = 59$).

Discussion

All of the right-handed patients in this study complained of left-hand pain, and the nondominant (right) precentral gyrus was stimulated electrically. Preoperative MR images and intraoperative somatosensory evoked potentials were used to determine the location of the central sulcus. Thus, we were able to precisely stimulate the area of the precentral gyrus corresponding to the left hand. We observed changes in neuronal activity with $H_2{}^{15}O$ PET, and all PET images were normalized and then analyzed using SPM.[7,8,9,15] Therefore, the results of this study were based on anatomically well-standardized samples and equal stimulation of identical brain regions.

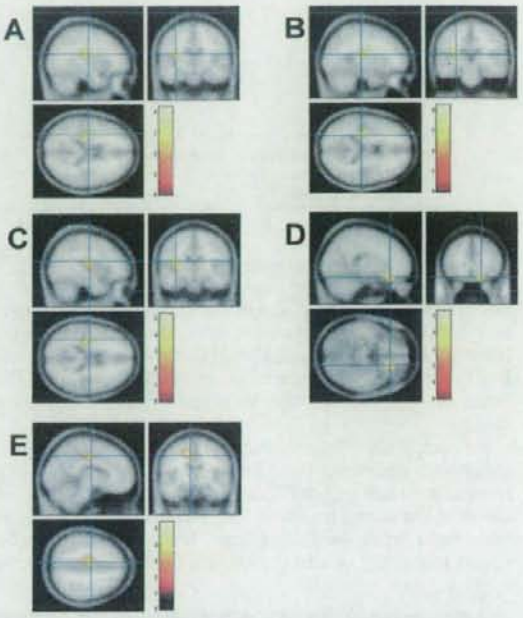

FIG. 1. Representative SPM (Z) intensity maps in normalized images. Comparison of rCBF before and after MCS showed that rCBF was increased after MCS in the left posterior insula (A) and left posterior thalamus (B). Comparison of rCBF before MCS and in the early post-MCS phase showed that rCBF was increased in the early post-MCS phase in the left posterior insula (C) and right orbitofrontal cortex (BA 11) (D). Comparison of rCBF before MCS and in the late post-MCS phase showed that rCBF was increased in the late post-MCS phase in the left ACC (E). The *colored bars* indicate the Z values; ($p < 0.005$).

TABLE 2

Areas of increased rCBF after MCS

Condition & Areas	Cluster		Talairach Coordinates (x, y, z in mm)	Voxel Equivalent Z
	p Value (corrected)	Size (voxel)		
pre-MCS compared w/ all phases of post-MCS				
lt insula	0.044	685	−31, −19, 15	3.57
lt thalamus			−25, −26, 11	3.38
pre-MCS compared w/ early phase of post-MCS				
lt insula	0.011	593	−33, −19, 15	4.44
rt orbitofrontal cortex (BA 11)	0.047	420	15, 26, −15	4.32
pre-MCS compared w/ late phase of post-MCS				
lt cingulate cortex (BA 24)	0.005	406	−8, −15, 38	4.47

TABLE 3
Areas of decreased rCBF after MCS

Condition & Areas	Cluster		Talairach Coordinates (x, y, z in mm)	Voxel Equivalent Z
	p Value (corrected)	Size (voxel)		
pre-MCS compared w/ early phase of post-MCS				
rt prefrontal cortex (BA 9)	0.048	406	29, 16, 29	4.10
rt precentral cortex (BA 4)			22, −11, 48	3.48

In this study, neither sham stimulation nor a control study was indicated. We used test stimulations of 10 to 14 days prior to the second surgery. Patients who had showed no effect or sham effect were excluded. And all of the patients in this study had used MCS for at least 6 months and had confirmed the effectiveness of MCS. We believe that there was no placebo effect associated with MCS in these cases.

It is not clear whether electrical stimulation activates or suppresses neurons around the point of stimulation. Some researchers have reported that low-frequency (5 Hz) stimulation of the cortex results in long-term potentiation of corticostriatal neuron activity in rats,[2] but the relationship between frequency of stimulation and effect on surrounding neurons has not been clarified. In our study, all patients showed the most pain reduction at frequencies between 25 and 40 Hz. Thus, we conclude that 25 to 40 Hz is a suitable range for MCS treatment of intractable pain. We found that stimulation in this frequency range decreased rCBF in the M1 for at least 20 minutes after MCS, indicating that the level of electrical stimulation used in this study inhibits neuronal activity under the electrode.

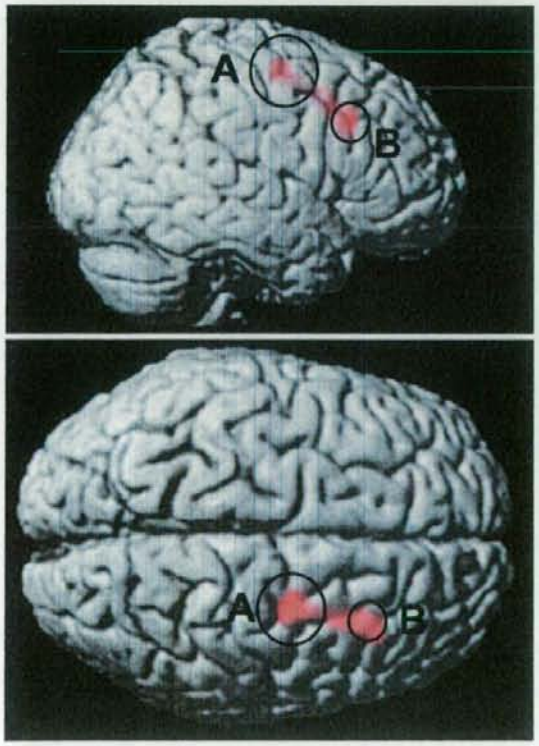

FIG. 2. Normalized images showing regions of significantly decreased rCBF in the early post-MCS phase compared to rCBF before MCS. *A* indicates the area of the precentral cortex (BA 4) and *B* the area of the dorsolateral prefrontal cortex (BA 9); ($p < 0.005$).

In this study, MCS did not alter rCBF in the postcentral gyrus (primary sensory cortex). This finding supports reports that MCS-induced pain reduction does not involve normal sensory pathways.[10,26] In fact, Drouot et al.[5] reported that MCS for control of chronic pain improves abnormal sensory thresholds. Thus, relief of chronic pain by MCS does not depend on sensory suppression and does not involve neuronal activity of the primary sensory cortex.

The rCBF in the right dorsolateral prefrontal cortex (BA 9) was also decreased after MCS. The prefrontal cortex is considered to include attentional and memory networks activated by noxious stimulation.[23,27] Lorenz et al.[18] also reported that BA 9 exerts active control of pain perception by modulating corticosubcortical and corticocortical pathways. Furthermore, repetitive transcranial magnetic stimulation of BA 9 has been reported to be effective in the treatment of depression.[6] Reduced BA 9 neuronal activity in the early post-MCS phase may reflect attenuation of attention and perception of chronic pain and may control psychological state.

The left posterior insula was activated in the early post-MCS phase. The posterior insula as well as the secondary somatosensory cortex are well described as reflecting pain perception and are parametrically activated by nociceptive input.[23,25,27,33,40] It was recently reported that in the rostral agranular insula, γ-aminobutyric acid can alter pain thresholds in rats and that locally increasing the level of this neurotransmitter in the insula induces analgesia by enhancing descending inhibition of spinal nociceptive neurons.[12] The posterior insula has connections to the periaqueductal gray matter, the area around the locus caeruleus, the rostroventral medulla, and the mesolimbic/mesocortical ventral forebrain.[11] Schlereth et al.[31] speculated that the left dorsal insula plays a dominant role in the early sensory-discriminative phase of pain processing. Thus, MCS appears to activate the left dominant posterior insula, resulting in upregulation of the pain threshold.

We found significantly increased rCBF in the right orbitofrontal cortex in the early post-MCS phase. Jasmin et al.[11] reported that the rostral agranular insula possesses reciprocal connections with the orbital infralimbic cortex and ACC in rats. It has also been reported that the cingulofrontal cortex, including the orbitofrontal cortex and the ACC in the area around the genu of the corpus callosum, exerts

a topdown influence on the posterior thalamus and periaqueductal gray matter to gate pain modulation during distraction.[40] The left posterior thalamus was activated in the early post-MCS phase in our study. Thus, it is possible that the activated orbitofrontal cortex, together with the posterior insula, excites the dominant posterior thalamus to upregulate the pain threshold.

The area of rCBF increase included the pulvinar of the thalamus (according to the atlas of Talairach and Tournoux[35]). In the 1970s, the posterior thalamus (pulvinar) was a target of lesioning surgery for cancer pain, and pulvinotomy resulted in early relief of cancer pain in most patients, but the pain often recurred.[37] Although the function of the posterior thalamus is not well characterized, we speculate that the dominant posterior thalamus is involved in chronic deafferentation pain.

Garcia-Larrea et al.[10] reported that the ipsilateral motor thalamus (ventrolateral and ventroanterior thalamus) and brainstem regions are activated by MCS. The ipsilateral thalamus shows hypometabolism in cases of central pain.[4,16] In our study, the ipsilateral (right) thalamus was not affected. In addition, one patient had poststroke pain but not severe motor dysfunction; others in this study had brainstem, spinal cord, or peripheral nerve injuries. Thus, corticostriatothalamic connections relating to movements were preserved in all patients, resulting in preserved right motor thalamus function.

The posterior insula projects efferent fibers to the amygdala in rats.[11] The bilateral caudal ACC and the posterior insula/secondary somatosensory cortex have been reported to be specific to the experience of pain.[1,33] It has also been reported that the caudal part of the right ACC is activated when the right M1 is stimulated magnetically in a capsaicin-induced pain model,[36] and the ACC is also activated by thalamic stimulation in patients with chronic pain.[3] The amygdala and cingulate gyrus belong to the limbic system and play important roles in emotional control. The caudal ACC (BA 24) contains the cingulate motor area,[32] which is associated with emotional behavior.[41] Our data showed that not only the posterior insula but also the caudal ACC (BA 24) were activated in response to MCS. Thus, MCS for treatment of chronic deafferentation pain modulates pain-related emotion and mood, resulting in pain relief. The caudal ACC, which was activated in the late post-MCS phase, contributes to long-lasting pain relief (several hours of relief) induced by MCS.

Conclusions

The use of MCS for the treatment of deafferentation upregulates the pain threshold by modulating pathways from the posterior insular and orbitofrontal cortex to the posterior thalamus. Treatment with MCS also controls pain-related emotion by modulating the pathway from the posterior insula to the caudal ACC. These findings support the use of MCS for treatment of deafferentation pain.

References

1. Botvinick M, Jha AP, Bylsma LM, Fabian SA, Solomon PE, Prkachin KM: Viewing facial expressions of pain engages cortical areas involved in the direct experience of pain. **Neuroimage 25:**312–319, 2005
2. Charpier S, Mahon S, Deniau JM: In vivo induction of striatal long-term potentiation by low-frequency stimulation of the cerebral cortex. **Neuroscience 91:**1209–1222, 1999
3. Davis KD, Taub E, Duffner F, Lozano AM, Tasker RR, Houle S, et al: Activation of the anterior cingulate cortex by thalamic stimulation in patients with chronic pain: a positron emission tomography study. **J Neurosurg 92:**64–69, 2000
4. De Salles AA, Bittar GT Jr: Thalamic pain syndrome: anatomic and metabolic correlation. **Surg Neurol 41:**147–151, 1994
5. Drouot X, Nguyen JP, Peschanski M, Lefaucheur JP: The antalgic efficacy of chronic motor cortex stimulation is related to sensory changes in the painful zone. **Brain 125:**1660–1664, 2002
6. Fitzgerald PB, Brown TL, Marston NAU, Daskalakis ZJ, de Castella A, Kulkarni J: Transcranial magnetic stimulation in the treatment of depression: a double-blind, placebo-controlled trial. **Arch Gen Psychiatry 60:**1002–1008, 2003
7. Friston KJ, Ashburner J, Poline JB, Frith CD, Heather JD, Frackowiak RSJ: Spatial registration and normalization of images. **Human Brain Mapp 2:**165–189 1995
8. Friston KJ, Frith CD, Liddle PF, Frackowiak RS: Comparing functional (PET) images: the assessment of significant change. **J Cereb Blood Flow Metab 11:**690–699, 1991
9. Friston KJ, Holmes AP, Worsley KJ, Poline JP, Frith CD, Frackowiak RSJ: Statistical parametric maps in functional imaging: a general linear approach. **Human Brain Mapp 2:**189–210, 1995
10. Garcia-Larrea L, Peyron R, Mertens P, Gregoire MC, Lavenne F, Le Bars D, et al: Electrical stimulation of motor cortex for pain control: a combined PET-scan and electrophysiological study. **Pain 83:**259–273, 1999
11. Jasmin L, Burkey AR, Granato A, Ohara PT: Rostral agranular insular cortex and pain areas of the central nervous system: a tract-tracing study in the rat. **J Comp Neurol 468:**425–440, 2004
12. Jasmin L, Rabkin SD, Granato A, Boudah A, Ohara PT: Analgesia and hyperalgesia from GABA-mediated modulation of the cerebral cortex. **Nature 424:**316–320, 2003
13. Kapur S, Meyer J, Wilson AA, Houle S, Brown GM: Activation of specific cortical regions by apomorphine: an [15O]H2O PET study in humans. **Neurosci Lett 176:**21–24, 1994
14. Katayama Y, Yamamoto T, Kobayashi K, Kasai M, Oshima H, Fukaya C: Motor cortex stimulation for post-stroke pain: comparison of spinal cord and thalamic stimulation. **Stereotact Funct Neurosurg 77:**183–186, 2001
15. Kiebel SJ, Ashburner J, Poline JB, Friston KJ: MRI and PET coregistration—a cross validation of statistical parametric mapping and automated image registration. **Neuroimage 5:**271–279, 1997
16. Laterre EC, De Volder AG, Goffinet AM: Brain glucose metabolism in thalamic syndrome. **J Neurol Neurosurg Psychiatry 51:** 427–428, 1998
17. Lorenz J, Garcia-Larrea L: Contribution of attentional and cognitive factors to laser evoked brain potentials. **Neurophysiol Clin 33:**293–301, 2003
18. Lorenz J, Minoshima S, Casey KL: Keeping pain out of mind: the role of the dorsolateral prefrontal cortex in pain modulation. **Brain 126:**1079–1091, 2003
19. Meyerson BA, Lindblom U, Linderoth B, Lind G, Herregodts P: Motor cortex stimulation as treatment of trigeminal neuropathic pain. **Acta Neurochir Suppl 58:**150–153, 1993
20. Mima T, Oga T, Rothwell J, Satow T, Yamamoto J, Toma K, et al: Short-term high-frequency transcutaneous electrical nerve stimulation decreases human motor cortex excitability. **Neurosci Lett 355:**85–88, 2004
21. Nguyen JP, Keravel Y, Feve A, Uchiyama T, Cesaro P, Le Guerinel C, et al: Treatment of deafferentation pain by chronic stimulation of the motor cortex: report of a series of 20 cases. **Acta Neurochir Suppl 68:**54–60, 1997
22. Nguyen JP, Lefaucheur JP, Decq P, Uchiyama T, Carpentier A, Fontaine D, et al: Chronic motor cortex stimulation in the treat-

ment of central and neuropathic pain. Correlations between clinical, electrophysiological and anatomical data. **Pain 82:**245–251, 1999
23. Ohara S, Crone NE, Weiss N, Lenz FA: Attention to a painful cutaneous laser stimulus modulates electrocorticographic event-related desynchronization in humans. **Clin Neurophysiol 115:** 1641–1652, 2004
24. Ostrowsky K, Magnin M, Ryvlin P, Isnard J, Guenot M, Mauguiere F: Representation of pain and somatic sensation in the human insula: a study of responses to direct electrical cortical stimulation. **Cereb Cortex 12:**376–385, 2002
25. Peyron R, Frot M, Schneider F, Garcia-Larrea L, Mertens P, Barral FG, et al: Role of operculoinsular cortices in human pain processing: converging evidence from PET, fMRI, dipole modeling, and intracerebral recordings of evoked potentials. **Neuroimage 17:**1336–1346, 2002
26. Peyron R, Garcia-Larrea L, Deiber MP, Cinotti L, Convers P, Sindou M, et al: Electrical stimulation of precentral cortical area in the treatment of central pain: electrophysiological and PET study. **Pain 62:**275–286, 1995
27. Peyron R, Laurent B, Garcia-Larrea L: Functional imaging of brain responses to pain. A review and meta-analysis. **Neurophysiol Clin 30:**263–288, 2000
28. Pioli EY, Gross CE, Meissner W, Bioulac BH, Bezard E: The deafferented nonhuman primate is not a reliable model of intractable pain. **Neurol Res 25:**127–129, 2003
29. Saitoh Y, Osaki Y, Nishimura H, Hirano S, Kato A, Hashikawa K, et al: Increased regional cerebral blood flow in the contralateral thalamus after successful motor cortex stimulation in a patient with poststroke pain. **J Neurosurg 100:**935–939, 2004
30. Saitoh Y, Shibata M, Hirano S, Hirata M, Mashimo T, Yoshimine T: Motor cortex stimulation for central and peripheral deafferentation pain. Report of eight cases. **J Neurosurg 92:**150–155, 2000
31. Schlereth T, Baumgartner U, Magerl W, Stoeter P, Treede RD: Left-hemisphere dominance in early nociceptive processing in the human parasylvian cortex. **Neuroimage 20:**441–454, 2003
32. Shima K, Tanji J: Role for cingulate motor area cells in voluntary movement selection based on reward. **Science 282:**1335–1338, 1998
33. Singer T, Seymour B, O'Doherty J, Kaube H, Dolan RJ, Frith CD: Empathy for pain involves the affective but not sensory components of pain. **Science 303:**1157–1162, 2004
34. Son BC, Kim MC, Moon DE, Kang JK: Motor cortex stimulation in a patient with intractable complex regional pain syndrome Type II with hemibody involvement. Case report. **J Neurosurg 98:**175–179, 2003
35. Talairach J, Tournoux P: **Co-Planar Stereotaxic Atlas of the Human Brain: 3-dimensional Proportional System: An Approach to Cerebral Imaging.** Stuttgart: Thieme, 1988
36. Tamura Y, Okabe S, Ohnishi T, N Saito D, Arai N, Mochio S, et al: Effects of 1-Hz repetitive transcranial magnetic stimulation on acute pain induced by capsaicin. **Pain 107:**107–115, 2004
37. Tasker RR: Stereotactic surgery, in Wall PD, Melzack R (eds): **Textbook of Pain, ed 3.** New York: Churchill Livingstone, 1994, pp 1137–1157
38. Tsubokawa T, Katayama Y, Yamamoto T, Hirayama T, Koyama S: Chronic motor cortex stimulation for the treatment of central pain. **Acta Neurochir Suppl 52:**137–139, 1991
39. Tsubokawa T, Katayama Y, Yamamoto T, Hirayama T, Koyama S: Chronic motor cortex stimulation in patients with thalamic pain. **J Neurosurg 78:**393–401, 1993
40. Valet M, Sprenger T, Boecker H, Willoch F, Rummeny E, Conrad B, et al: Distraction modulates connectivity of the cingulo-frontal cortex and the midbrain during pain—an fMRI analysis. **Pain 109:**399–408, 2004
41. Vogt BA, Berger GR, Derbyshire SW: Structural and functional dichotomy of human midcingulate cortex. **Eur J Neurosci 18:** 3134–3144, 2003
42. Wang JY, Zhang HT, Han JS, Chang JY, Woodward DJ, Luo F: Differential modulation of nociceptive neural responses in medial and lateral pain pathways by peripheral electrical stimulation: a multichannel recording study. **Brain Res 1014:**197–208, 2004
43. Wood CC, Spencer DD, Allison T, McCarthy G, Williamson PD, Goff WR: Localization of human sensorimotor cortex during surgery by cortical surface recording of somatosensory evoked potentials. **J Neurosurg 68:**99–111, 1988

Manuscript submitted July 2, 2006.
Accepted September 19, 2006.
Address reprint requests to: Youichi Saitoh, M.D., Ph.D., Department of Neurosurgery, Osaka University Graduate School of Medicine, 2-2 Yamadaoka, Suita, Osaka, 565-0871, Japan. email: neurosaitoh@mbk.nifty.com.

European Journal of Endocrinology (2007) 157 265–270 ISSN 0804-4643

CLINICAL STUDY

Reduced epinephrine reserve in response to insulin-induced hypoglycemia in patients with pituitary adenoma

Shinya Morita[1], Michio Otsuki[1], Maki Izumi[1], Nobuyuki Asanuma[1], Shuichi Izumoto[2], Youichi Saitoh[2], Toshiki Yoshimine[2] and Soji Kasayama[1]

Department of [1]Medicine and [2]Neurosurgery, Osaka University Graduate School of Medicine (C-4), 2-2 Yamada-oka, Suita, Osaka 565-0871, Japan

(Correspondence should be addressed to S Kasayama; Email: kasayama@imed3.med.osaka-u.ac.jp)

Abstract

Objective: Hypoglycemia induces rapid secretion of counterregulatory hormones such as catecholamine, glucagon, cortisol, and GH. Insulin-induced hypoglycemia is used for evaluating GH–IGF-I and ACTH–adrenal axes in patients with pituitary disorders. The aim of this study was to determine whether the response of catecholamine secretion to hypoglycemia is disrupted in patients with pituitary adenoma.

Methods: The study population comprised 23 patients with pituitary adenoma (non-functioning adenoma or prolactinoma). An insulin tolerance test was performed and serum catecholamines as well as plasma GH and serum cortisol were measured.

Results: The study patients showed diminished response of plasma epinephrine to insulin-induced hypoglycemia. With the cutoff level of peak epinephrine for defining severe impairment set at 400 pg/ml, more patients with secondary adrenal insufficiency showed severe impairment of the epinephrine response than did those without it. Peak epinephrine levels to insulin-induced hypoglycemia were significantly correlated with peak cortisol levels. In patients with secondary hypothyroidism, secondary hypogonadism, GH deficiency, or diabetes insipidus, the prevalence of severe impairment of the epinephrine response was similar to that in patients without these deficiencies.

Conclusions: Impaired epinephrine secretion in response to insulin-induced hypoglycemia was frequently observed in patients with pituitary adenoma. This disorder was especially severe in patients with secondary adrenal insufficiency.

European Journal of Endocrinology **157** 265–270

Introduction

Glucose counterregulatory mechanisms in response to hypoglycemia consist of rapid secretion of adrenocorticotropin (ACTH), growth hormone (GH), glucagon, epinephrine, and norepinephrine (1, 2). In patients with type 1 diabetes mellitus, insulin treatment increases the risk of severe hypoglycemia (3). In addition, defective glucose counterregulation is sometimes associated with diabetic patients, and becomes a cause for hypoglycemia unawareness (4), while single or recurrent episodes of hypoglycemia have been shown to impair sympathoadrenal responses to a subsequent episode of hypoglycemia (5, 6). Moreover, patients with insulinoma often also have a lowered glycemic threshold for the activation of glucose counterregulation (7).

The brain ventromedial hypothalamus (VMH) has been shown to sense hypoglycemia and trigger the release of counterregulatory hormones (8–12). Corticotropin-releasing hormone (CRH) acting via CRH receptor 1 has been found to play an important role in the sympathoadrenal downregulation in a rodent model of antecedent hypoglycemia (13). It has further been reported that a patient with hypothalamic sarcoidosis suffered complete loss of the counterregulatory response to hypoglycemia as well as pituitary insufficiency and central diabetes insipidus (14). In addition, pediatric and adult patients with craniopharyngioma have been shown to have a defect in sympathoadrenal counterregulation (15, 16). However, it is not known whether the counterregulatory response of catecholamines to hypoglycemia is disrupted in patients with pituitary adenomas. Therefore, we studied the responses of catecholamine secretion in response to insulin-induced acute hypoglycemia in patients with pituitary adenoma, who had a variety of hypothalamic–pituitary hormone disorders.

Patients and methods

Patients

The study population consisted of 23 patients with diagnosed pituitary adenoma. Among 90 such patients visiting Osaka University Hospital between December 2003 and January 2007, the study patients were randomly selected after exclusion of patients with ACTH- or GH-producing adenoma. Seven patients

DOI: 10.1530/EJE-07-0176
Online version via www.eje-online.org

were males and sixteen females, their mean age at the time of this study was 55 years (range, 20–76 years), and their body mass index was 24.3 ± 2.9 kg/m^2. Eighteen patients had clinically non-functioning adenomas and five patients had prolactinomas. The diagnosis of these tumors was made by enhanced magnetic resonance imaging and was confirmed by transsphenoidal surgery or craniotomy in 21 of the patients. Table 1 shows the clinical characteristics of the study population. All patients gave their informed consent, and the investigation was performed in accordance with the principles of the Declaration of Helsinki as revised in 2000.

Endocrine evaluation

All patients were hospitalized. Endocrine evaluation tests were performed between 0800 and 1000 h. All medications were allowed to be taken after the endocrine evaluation tests ended. After a 15 min rest, regular insulin (0.1 unit/kg body weight) was administered intravenously in a single injection. Blood samples were obtained for measurements of pituitary hormones, cortisol, epinephrine, and norepinephrine at the time of injection, and 15, 30, 60, 90, and 120 min after the injection. When hypoglycemia (blood glucose levels <40 mg/dl or half of basal levels) was not obtained within 30 min after the insulin injection, an additional 0.05 unit/kg body weight of insulin was injected to induce hypoglycemia. During the endocrine tests, the patients were keeping spine position.

Secondary adrenal insufficiency was diagnosed if the peak serum cortisol response was <200 μg/l during the insulin tolerance test (ITT) (17, 18) and if early morning (0800 h) serum cortisol levels were <80 μg/l and 24-h urinary-free cortisol levels were low (<30 μg/24 h). Secondary hypothyroidism was indicated by low free L-thyroxine (T_4) concentrations (<8 ng/l) with normal or low thyrotropin (TSH) levels (1, 2). Secondary hypogonadism was identified in premenopausal women by menstrual disturbances, low estradiol levels (<20 pg/ml) with normal or low follicle-stimulating hormone (FSH) and luteinizing hormone (LH) levels, and in postmenopausal women by relatively low FSH and LH levels. In men, secondary hypogonadism was indicated by low testosterone levels (<3 μg/l) with low or normal FSH and LH levels (17, 18). A diagnosis of GH deficiency was based on a peak GH response of <5 μg/l at ITT (17, 18), and a diagnosis of diabetes insipidus on the presence of a markedly large dilute urine volume (>2.5–3 l per 24 h) with low urine osmolality (<300 mmol/kg) (17, 18). Patients who had been diagnosed with secondary adrenal insufficiency, secondary hypothyroidism, and/or diabetes insipidus had been receiving replacement therapy with appropriate doses of hydrocortisone, T_4, and/or desmopressin. No patient with GH deficiency had

Table 1 Type and size of pituitary adenoma, defective pituitary hormones, replaced hormones therapy, and previous surgery in the study population.

Patient no	Age/sex	Hormone produced	Size of tumor (mm)	Defective pituitary hormone(s)	Replaced hormone(s)	Duration of replacement therapy	Previous surgery
1	21/M	NF	22	ACTH, GH, TSH, LH/FSH, AVP	H, T_4, DDAVP	60 months	TSS, craniotomy
2	31/F	NF	30	None	None		None
3	50/F	NF	23	GH, TSH, LH/FSH, AVP	DDAVP	1 month	None
4	56/F	NF	38	ACTH, GH, TSH, LH/FSH	None		TSS
5	56/F	NF	32	GH, LH/FSH	None		TSS
6	57/F	NF	12	GH	None		None
7	58/F	NF	25	GH, TSH, LH/FSH	None		None
8	58/F	NF	29	GH, TSH, LH/FSH	T_4	60 months	TSS
9	59/F	NF	26	ACTH, GH	None		None
10	62/M	NF	25	GH, LH/FSH	None		None
11	62/M	NF	24	GH	None		None
12	62/F	NF	70	GH	None		Craniotomy
13	65/F	NF	13	ACTH, GH, TSH, LH/FSH	H, T_4	1 month	None
14	71/M	NF	38	ACTH, GH, TSH	H	1 month	None
15	72/F	NF	32	LH/FSH	None		TSS
16	74/M	NF	18	GH, LH/FSH	Tes	12 months	TSS
17	75/M	NF	28	ACTH, GH, TSH, LH/FSH	None		None
18	76/F	NF	31	GH, TSH, LH/FSH, AVP	DDAVP	1 month	TSS
19	20/F	Prolactin	21	LH/FSH	None		None
20	30/F	Prolactin	13	LH/FSH	None		None
21	43/F	Prolactin	11	LH/FSH	None		None
22	53/M	Prolactin	20	LH/FSH	None		None
23	62/F	Prolactin	23	ACTH, GH, LH/FSH	None		None

NF, non-functioning; DDAVP, desmopressin; H, hydrocortisone; T_4, L-thyroxine; Tes, testosterone; TSS, transsphenoidal surgery. The size of the tumor is shown as the maximal diameter.

received GH replacement therapy, and only one male patient with secondary hypogonadism had received testosterone replacement.

Hormone assays

All hormones were assayed in the Clinical Laboratory of Osaka University Hospital. GH, ACTH, free T_4, free triiodothyronine, and cortisol were measured by means of RIA. Prolactin, LH, and FSH were measured by means of enzyme-immunoassay, TSH by electrochemiluminescence immunoassay, epinephrine and norepinephrine by high performance liquid chromatography, and plasma glucose with the glucose oxidase method.

Statistical analysis

Peak epinephrine secretion of patients with different pituitary hormone disorders was compared using the χ^2 test. The StatView computer program (Version 5.0 for Windows; Abacus Concepts, Berkeley, CA, USA) was used for statistical analyses. $P<0.05$ was considered statistically significant.

Results

Subjects

Table 1 shows characteristics of the tumors, defective pituitary hormones, replaced hormones therapy, and previous surgery in the study population. The maximal diameter of the tumors ranged from 11 to 70 mm. Out of the 23 patients, 22 had anterior and/or posterior pituitary hormones deficiencies; four patients showed signs of panhypopituitarism, and three of central diabetes insipidus. All five patients with prolactinoma had hypogonadism. Three patients had been receiving hydrocortisone at 10 or 20 mg daily after breakfast, while three patients had been receiving T_4 at 25 or 75 μg daily after breakfast. No patient had DHEA replacement therapy. Desmopressin had been administered to three patients with central diabetes insipidus. Eight of the study patients had previously received transsphenoidal surgery or craniotomy. There were no patients with prolactinoma who had been treated with dopamine agonist.

Catecholamines responses to insulin-induced hypoglycemia

Plasma epinephrine and norepinephrine responses to ITT are shown in Fig. 1. Baseline plasma epinephrine levels were within control ranges (<170 pg/ml) in all patients. However, all patients showed a diminished response of plasma epinephrine to insulin-induced hypoglycemia. Baseline plasma norepinephrine levels were considerably lower in five of the patients than in controls (150–570 pg/ml) and were within control ranges in the other 18 patients, while secretory responses of plasma norepinephrine were ambiguous.

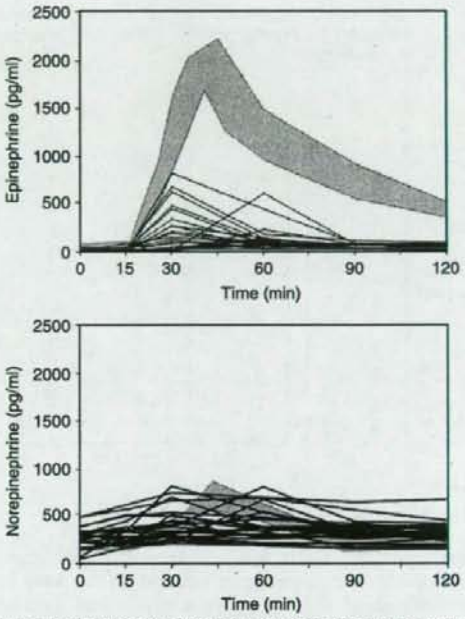

Figure 1 Epinephrine (top) and norepinephrine (bottom) responses to insulin-induced hypoglycemia in 23 patients with pituitary adenoma. The shaded area represents the mean ± S.E.M. values for normal subjects (Ref. (19)). To convert the values for epinephrine and norepinephrine to nanomoles per liter, multiply by 0.0005458 and 0.005910 respectively.

Relationship between epinephrine responses at ITT and defective pituitary hormones of the study patients

With the cutoff level of peak epinephrine at ITT for identifying severe impairment set at 400 pg/ml, more patients with secondary adrenal insufficiency showed severe impairment of the epinephrine response than those without it (Fig. 2 and Table 2). On the other hand, patients with secondary hypothyroidism, secondary hypogonadism, GH deficiency, and/or diabetes insipidus showed a similar prevalence of severe impairment of the epinephrine response as those without these abnormalities. Peak epinephrine levels at ITT were significantly correlated with peak cortisol levels ($R=0.506$, $P=0.014$; Fig. 3). In contrast, there was no correlation of the peak epinephrine levels with the peak GH levels ($R=0.072$, $P=0.745$) and the lowest plasma glucose levels ($R=-0.147$, $P=0.503$) at ITT.

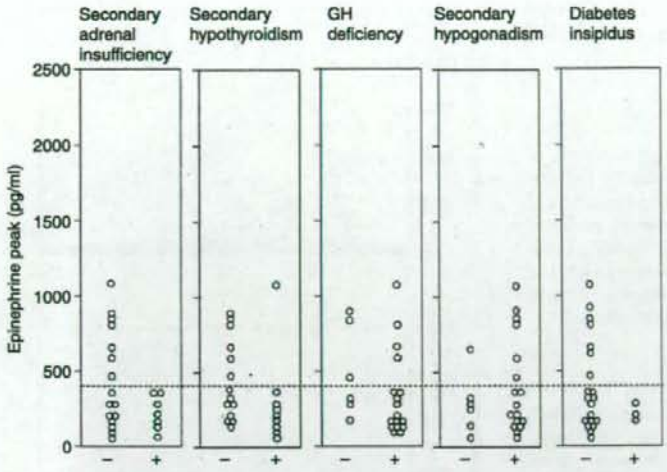

Figure 2 Peak epinephrine levels during the insulin tolerance test in 23 patients with pituitary adenoma. The patients were divided to subgroups according to pituitary hormonal deficiencies. To convert the values for epinephrine to nanomoles per liter, multiply by 0.0005458.

Discussion

Insulin-induced acute hypoglycemia is a well-known stimulus for the secretion of GH and ACTH from the pituitary gland (17, 18). This stimulus has therefore been used for the diagnosis of GH deficiency and secondary adrenal deficiency in patients with suspected hypopituitarism (17, 18). Besides GH and ACTH/cortisol, other counterregulatory hormones such as epinephrine, norepinephrine, and glucagon, also play pivotal roles in recovery from hypoglycemia (1, 2). Glucose counterregulation deficiency has been found to be associated with diabetes mellitus (3–5), insulinoma (7), hypothalamic sarcoidosis (14), craniopharyngioma (15, 16), and psychological stress (20). Deficiencies in glucose counterregulatory hormones have been shown to vary, depending on the background disease: responses of glucagon and GH were impaired in diabetic patients (21), those of GH, cortisol, glucagon, epinephrine, and norepinephrine in a patient with hypothalamic sarcoidosis (14), and those of cortisol, epinephrine, and norepinephrine in a patient with psychological stress (20). Of the 23 patients with pituitary adenoma enrolled in our study, all showed diminished plasma epinephrine response to insulin-induced acute hypoglycemia. Reduction in the epinephrine reserve thus occurred with very high frequency in these patients. Unfortunately, neuroglycopenic symptoms during insulin-induced hypoglycemia were not accurately recorded in some patients. Thus, in the present study, we failed to reveal the relationship between these symptoms and the diminished plasma epinephrine response.

Glucocorticoids are required for the survival and maintenance of adrenomedullary chromaffin cells and their production of epinephrine (22, 23). In fact, adrenomedullary hypofunction was observed in patients with 21-hydroxylase deficiency (24, 25) and those with isolated glucocorticoid deficiency (26). In these patients, plasma epinephrine concentrations at baseline and in response to stimuli such as exercise, upright posture and cold pressure, were reduced (24–26). Adrenomedullary dysfunction was characterized by incomplete formation of the adrenal medulla and a depletion of secretory vesicles in chromaffin cells (24). Basal and post-exercise plasma epinephrine levels were also found to be reduced in children with ACTH deficiency (27). In our study, peak epinephrine levels at ITT were correlated with peak cortisol levels, but not with peak GH levels. These results suggest that secondary adrenal insufficiency could be an important

Table 2 Prevalence of severe impairment of the epinephrine response to insulin-induced hypoglycemia.

Peak epinephrine level at ITT	<400 (pg/ml)	≥400 (pg/ml)	P
Secondary adrenal insufficiency			
(−)	9 (39%)	7 (30%)	0.036
(+)	7 (30%)	0 (0%)	
Secondary hypothyroidism			
(−)	8 (35%)	6 (26%)	0.106
(+)	8 (35%)	1 (4%)	
GH deficiency			
(−)	3 (13%)	3 (13%)	0.226
(+)	13 (57%)	4 (17%)	
Secondary hypogonadism			
(−)	5 (22%)	1 (4%)	0.394
(+)	11 (48%)	6 (26%)	
Diabetes insipidus			
(−)	13 (57%)	7 (30%)	0.219
(+)	3 (13%)	0 (0%)	

ITT, insulin tolerance test.